Defects in Microcontact-Printed and Solution-Grown Self-Assembled Monolayers

ARTICLE *in* LANGMUIR · FEBRUARY 1999

Impact Factor: 4.46 · DOI: 10.1021/la981067r

5 AUTHORS, INCLUDING:

Atul N Parikh
University of California, Davis
175 PUBLICATIONS **6,824** CITATIONS

SEE PROFILE

Langmuir
The ACS Journal of Surfaces and Colloids

MARCH 2, 1999
VOLUME 15, NUMBER 5

Letters

Defects in Microcontact-Printed and Solution-Grown Self-Assembled Monolayers

A. S. Eberhardt,* R. M. Nyquist, A. N. Parikh, T. Zawodzinski, and B. I. Swanson

Los Alamos National Laboratory, Los Alamos, New Mexico 87545

Received August 20, 1998. In Final Form: December 31, 1998

The structure of microcontact-printed self-assembled monolayers is significant for a number of technological applications as well as for a fundamental understanding of the self-assembly process. The structural differences between printed and solution-deposited monolayers of alkanethiol on Au(111) have been examined utilizing grazing incidence X-ray diffraction and atomic force microscopy. Although the local structures are found to be similar, the domain structure and therefore macroscopic packing of the molecules are found to vary. Surprisingly, printed decanethiol monolayers appear to be significantly better ordered translationally than those formed by standard solution techniques.

Introduction and Previous Work

Microcontact printing, a method for patterning multicomponent self-assembled monolayers developed at Harvard,[1] is scientifically and technologically useful for applications in such diverse areas as substrates for biologically relevant studies,[2] organic electronics,[3] microfabrication,[4] and chemical or biological sensing.[5] The molecular level structure of the film clearly affects these applications, particularly in terms of the film defects and tail group orientation. As patterned films are created by printing part of the monolayer and filling in the rest by solution deposition, any differences in the final structure between films formed by the two techniques acquire particular significance. Additionally, any structural variations must be understood for the utilization of chemical force microscopy, in which chemically modified tips are used to examine the local chemistry of a surface.[6] Several recent papers have compared the molecular structure of printed and solution-grown monolayers, some finding that the two are very similar or identical, as measured by scanning tunneling microscopy and wettability[7] or Fourier transform infrared spectroscopy (FTIR).[8] Another study, utilizing near edge X-ray absorption fine structure spectroscopy (NEXAFS), found that stamped monolayers were generally less well ordered than standard solution deposited films,[9] and differences ascribed to defect distribution were also observed with X-ray photoelectron spectroscopy.[10] Some atomic force microscopy (AFM) images indicate a subtle difference between stamped and solution-deposited regions of single-component monolayers, as expressed in the presence of contrast in the frictional image of lateral force microscopy (LFM) and the phase image of force modulation microscopy (FMM).[8] These differences

(1) Kumar, A.; Biebuyck, H. A.; Whitesides, G. M. *Langmuir* **1994**, *10*, 1498.
(2) (a) Mrksich, M.; Dike, L. E.; Tien, J.; Ingber, D. E.; Whitesides, G. M. *Exp. Cell Res.* **1997**, *235*, 305−13. (b) Bernard, A.; Delamarche, E.; Schmid, H.; Michel, B.; Bosshard, H. R.; Biebuyck, H. *Langmuir* **1998**, *14*, 2225−9.
(3) Jackman, R. J.; Rogers, J. A.; Whitesides, G. M. *IEEE Trans. Magn.* **1997**, *33*, 2501−3.
(4) Wilbur, J. L.; Kumar, A.; Biebuyck, H. A.; Kim, E.; Whitesides, G. M. *Nanotechnology* **1996**, *7*, 452−457.
(5) Mrksich, M.; Whitesides, G. M. *Trends Biotech.* **1995**, *13*, 228−235.
(6) (a) Frisbie, C. D.; Rozsnyai, L. F.; Noy, A.; Wrighton, M. S.; Lieber, C. M. *Science* **1994**, *265*, 2071−2074. (b) Noy, A.; Frisbie, C. D.; Rozsnyai, L. F.; Wrighton, M. S.; Lieber, C. M. *J. Am. Chem. Soc.* **1995**, *117*, 7943−7951.
(7) Larsen, N. B.; Biebuyck, H.; Delamarche, E.; Michel, B. *J. Am. Chem. Soc.* **1997**, *119*, 3017−3026.

10.1021/la981067r CCC: $18.00
Published on Web 02/11/1999

were ascribed to variations in the packing density of molecules in the two regimes, some of which may arise from issues involved in the transport of molecules from the stamp to the surface.[11] This contrast is at least partially explained here by observed differences in the domain sizes of stamped and solution-deposited layers, leading to differences in the molecular density due to line defects, while the local molecular structures appear to be similar or identical.

Experimental Methods

Decanethiol, nonanethiol, and hexadecanethiol were used as received from Aldrich (Aldrich Chemical Co., Inc., Milwaukee, WI). Solutions were made with dehydrated absolute ethanol from Quantum (Millenium Petrochemicals, IL). The solution grown films were created by exposing a gold substrate to a 1 mM solution of thiol in ethanol for ~10 min unless otherwise indicated. Preparation of stamped monolayers has been described elsewhere.[1,12] Briefly, an elastomeric (Sylgard 184, Dow Corning, MI) stamp was fabricated from a photoresist master and allowed to cure at 65 °C for at least 1 h and then overnight at room temperature. These were rinsed in heptane and ethanol, inked with a small amount of 1 mM thiol ethanol solution, dried, and placed in contact with the gold surface for 60 s. Inking the stamp was accomplished by immersing a clean cotton swab in solution and then brushing it lightly across the surface of the stamp to wet it, drying the stamp under a clean nitrogen flow after 15−30 s, and repeating the process twice more. Except where otherwise noted, the substrates were subsequently immersed for 10 min in a 1 mM solution identical to that used to ink the stamps.

The single-crystal Au(111) substrates were received (Aremco Products, Inc., NY), polished, and precleaned with a gold peroxide etch. GIXD measurements indicated miscuts of less than 0.4° across the 1.2 cm surface. These surfaces were initially cleaned and prepared utilizing argon ion sputtering and annealing in a vacuum (~10^{-7} Torr). They were then exposed to solution or a blank stamp and kept in an argon environment for up to 2 weeks before GIXD measurements at Brookhaven National Laboratory (BNL). For subsequent use, the crystals were flame-annealed in a propane torch to reclean the gold surface for further measurements. This was accomplished by placing the crystals on a thick tantalum foil or brick slab and exposing them to the torch flame in air until the sample was observed to glow; then they were allowed to cool slowly to room temperature before exposure to stamp or solution. No significant differences in gold or monolayer order were observed in the diffraction or AFM patterns utilizing the two preparation techniques, except that repeated annealing with the propane torch led to the formation of small crystallites on the surface, whose removal required the argon cleaning procedure or etch. AFM images were also taken on samples prepared on sputtered gold substrates. Gold (2000 Å) was deposited in a Perkin-Elmer sputter system at 10^{-6} to 10^{-7} Torr, on silicon coated with a thin adhesive layer of titanium.

GIXD measurements were performed at the ×22B beam line at the National Synchrotron Light Source at BNL, on a Huber four-circle diffractometer, as described in a previous publication.[13] The diffractometer was operated in the symmetric mode (incoming beam at the same incident angle as outgoing beam), with a small chamber serving as a clean environment for the sample. This utilized a beryllium window for X-ray transmission and was slightly overpressured with ultrapure helium. The diffraction signal was seen to degrade after 2−3 h due to X-ray damage. The data were taken with an incident 1.13 Å X-ray beam of size 0.5 mm horizontal × 1.0 mm vertical, at an incident angle varying from 0.8° to 8.2° and a vertical resolution of 0.03 $Å^{-1}$, set by slits before the sample and detector. The measurements themselves took only a few minutes, up to approximately half an hour for the complete rod scans. The rod scans shown here in Figure 1 were normalized to monitor intensities, by the Lorentz factor, by the out-of-plane detector resolution, and to the active sample area (that part of the sample both illuminated by the X-ray beam and visible to the detector).[14] Rod scans are a measure of the intensity variation along the diffuse rod of the diffraction intensity perpendicular to the plane of the monolayer (diffraction out of the page in the schematic of Figure 1A). The peak positions provide estimates for the tilt angle and tilt direction of the molecular backbone.[15]

The AFM characterization employed a Nanoscope IIIa from Digital Instruments in air, utilized in contact mode. Oxide-sharpened silicon nitride (NP-S from D.I.) tips were used with a force of approximately 15 nN for all images, as calculated from the provided force constant of the tip. All images were gathered under identical conditions.

Results and Discussion

A comparison of the GIXD structural information for stamped and solution grown monolayers indicates that the two molecular structures are identical. The same two-dimensional symmetry is observed in both systems, as represented in the schematic inset to Figure 1, showing the previously measured pattern and the inset superlattice diffraction peak.[13] Figure 1 also compares the structure out-of-plane for the two deposition techniques. The peak positions are observed to be close to 0.85 $Å^{-1}$ and less than 0.2 $Å^{-1}$, both within the error of previously quoted values, leading to a 33.5 ± 1° tilt in a direction halfway between the nearest and next nearest neighbors.[15] This conclusion also agrees with the previous STM and FTIR results that the two differently formed monolayers have the same molecular structure, despite the observed frictional contrast.[7,8] However, in contrast to the case of ref 7, no lower density phase was observed, such as the "striped" phase characteristic of a partially formed monolayer.[16] These may be difficult to observe with GIXD, as they were also not seen in studies of monolayer formation.[17]

In Figure 2A, transverse scans through the first-order diffraction peaks are compared for the two types of films. As the scans are in reciprocal space, the width of the peak is inversely proportional to the average coherence length of the monolayer. This translates directly to an average domain size, barring odd domain shapes. For the decanethiol monolayer, the average domain size of the stamped film is about 400 Å, while that of the solution-grown film is only 150 Å. Each domain is separated from the next by a change in tilt angle (a multiple of 60°) or a line defect in which the molecules are no longer in registry. Smaller domains thus imply that the molecules are more loosely packed and that these regions will be softer, leading to greater friction (lighter in the image), as suggested in ref 8. Figure 2B provides an overview of these domain sizes (assumed similar to the observed coherence length), as well as those of molecules stamped with a higher concentration solution, as suggested in ref 7. Monolayers grown or deposited on substrates prepared by flame annealing or UHV sputtering (which implies the film was deposited ahead of time and transported to BNL) are also indicated. Although there is some scatter, the points clearly fall into two domain regions, with no obvious effect from

(8) Bar, G.; Rubin, S.; Parikh, A. N.; Swanson, B. I.; Zawodzinski, T. A., Jr.; Whangbo, M.-H. *Langmuir* **1997**, *13*, 373−377.
(9) Fischer, D.; Marti, A.; Hahner, G. *J. Vac. Sci. Technol., A* **1997**, *15*, 2173−80.
(10) Evans, S. D.; Cooper, S. D.; Johnson, S. R.; Flynn, T. M.; Ulman, A. *Supramol. Sci.* **1997**, *4*, 247−52.
(11) Delamarche, E.; Schmid, H.; Bietsch, A.; Larsen, N. B.; Rothuizen, H.; Michel, B.; Biebuyck, H. J. *Phys. Chem. B* **1998**, *102*, 3324−34.
(12) (a) Kumar, A.; Whitesides, G. M. *Appl. Phys. Lett.* **1993**, *63*, 2002. (b) Bar, G.; Rubin, S.; Taylor, T. N.; Swanson, B. I.; Zawodzinski, T. A., Jr.; Chow, J. T.; Ferraris, J. P. *J. Vac. Sci. Technol., A* **1996**, *14*, 1794.
(13) Fenter, P.; Eberhardt, A.; Eisenberger, P. *Science* **1994**, *266*, 1216−1218.
(14) Robinson, I. K. *Aust. J. Phys.* **1988**, *41*, 359−67.
(15) Fenter, P.; Eberhardt, A.; Liang, K. S.; Eisenberger, P. *J. Chem. Phys.* **1997**, *106*, 1600.
(16) Poirier, G. E.; Pylant, E. D. *Science* **1996**, *272*, 1145.

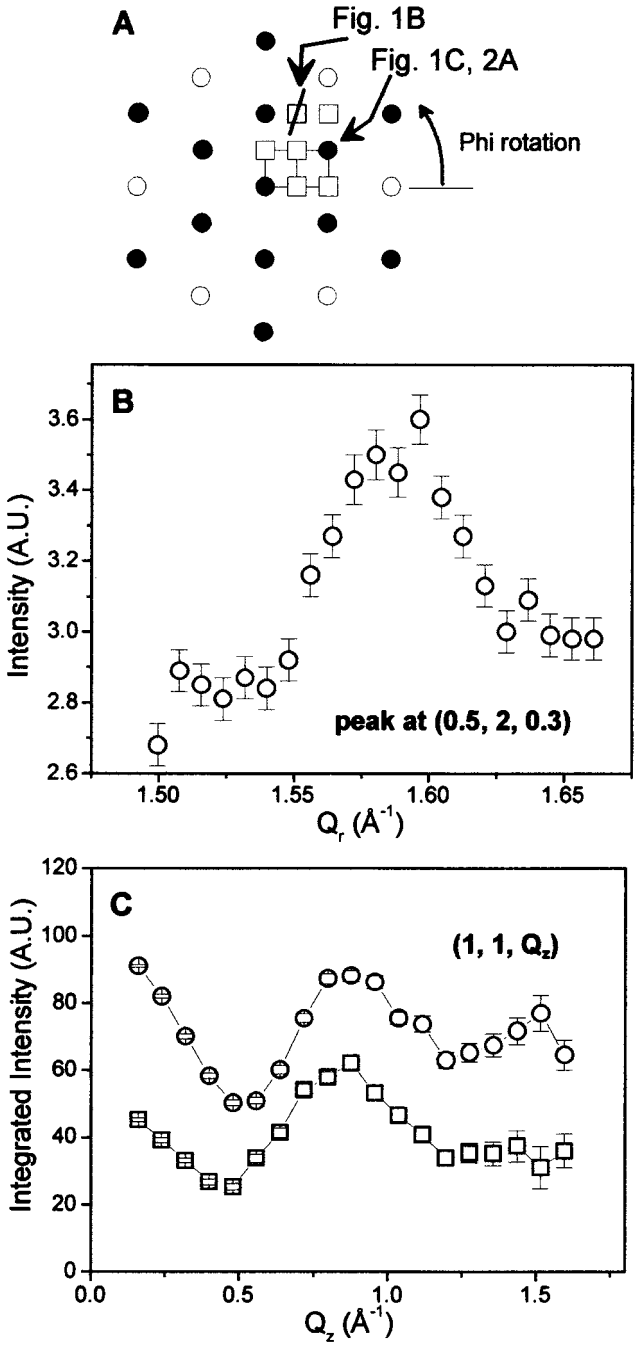

Figure 1. Molecular structure of stamped monolayers. The figure illustrates the monolayer structure for both stamped (circle) and solution-deposited (square) decanethiol monolayers. Part A is a schematic of the two-dimensional diffraction pattern observed parallel to the monolayer substrate. The open circles correspond to diffraction from the gold substrate, the closed to diffraction from a hexagonally ordered overlayer, and the squares to a rectangular superlattice distortion of this hexagonal symmetry. The dark circle whose diffraction is shown in part C and Figure 2A is at (1,1) in units of inverse angstroms (h = 1.257, k = 0.725, l = 2.667). The radial scan through the indicated superlattice peak is shown in part B. The rod scans are generated by a series of transverse (phi) scans at different heights above the sample, in the first-order hexagonal position indicated, as shown in Figure 2A. The total intensity in each transverse scan is plotted in part C. The existence of the same superlattice symmetry in the solution-grown and stamped monolayers and the similar tilt angles derived from the rod scans imply that the local structures are similar.

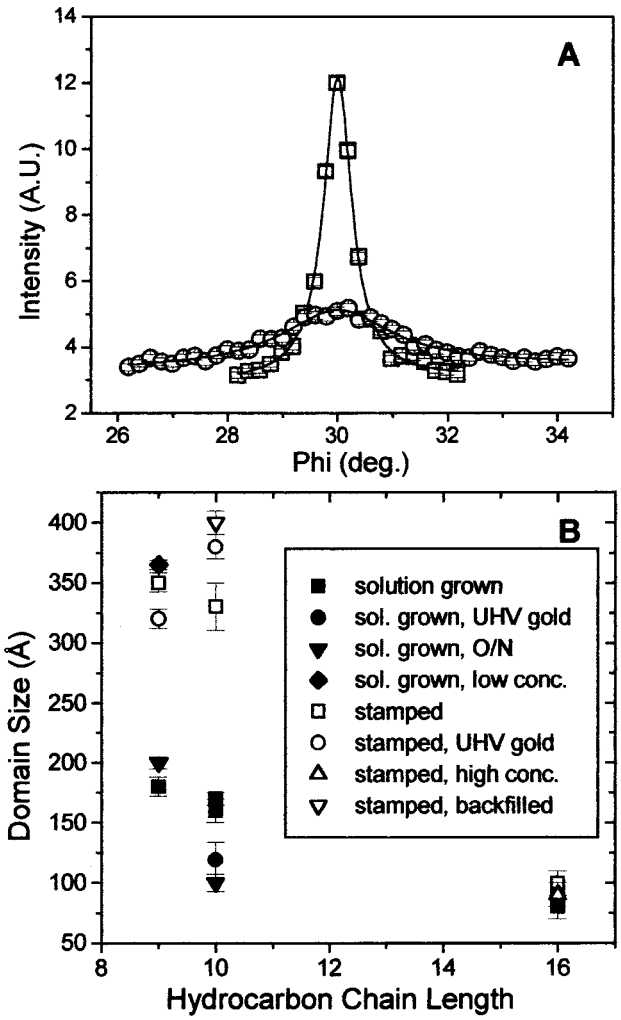

Figure 2. Domain sizes of stamped monolayers. The scans in part A are through the peak indicated in Figure 1; the width is an average for the monolayer over the whole surface. The narrow peak indicated with squares is from a stamped nonanethiol monolayer, and the wider peak indicated with circles is from a solution-grown monolayer; both are fit to single Lorentzian line shapes. The narrower the peak in reciprocal space (diffraction), the larger the coherence length in real space. Part B provides an overview of domain sizes for different hydrocarbon chain lengths and deposition techniques. The open symbols refer to stamped monolayers, and the closed symbols refer to solution-deposited monolayers. The squares represent samples prepared by the standard methodology on flame-annealed substrates. The circles refer to samples prepared at LANL on surfaces cleaned in UHV. The filled down triangles are for monolayers prepared in solution overnight; while the open down triangles refer to stamped blank surfaces which were subsequently backfilled by exposing them to the solution. The open up triangles were stamped with much higher concentration solutions as in ref 7, while the sample marked with a closed diamond was grown from a 1 μM solution. The hexadecanethiol samples were stamped normally, stamped with high concentrations, and solution grown on both annealed and UHV-prepared substrates. The error bars refer to the measurement error only.

the other varied parameters, including length of substrate immersion. There is one exception: a nonanethiol monolayer grown from a very dilute solution has an extremely large domain size. On the other hand, the hexadecane films show no such separation by growth mode, possibly because the more complex phase diagram associated with longer chain molecules alters the monolayer formation kinetics.[17−19] In all cases, the surface gold was found to

(17) Eberhardt, A.; Fenter, P.; Eisenberger, P. *Surf. Sci.* **1998**, *397*, L285−L290.

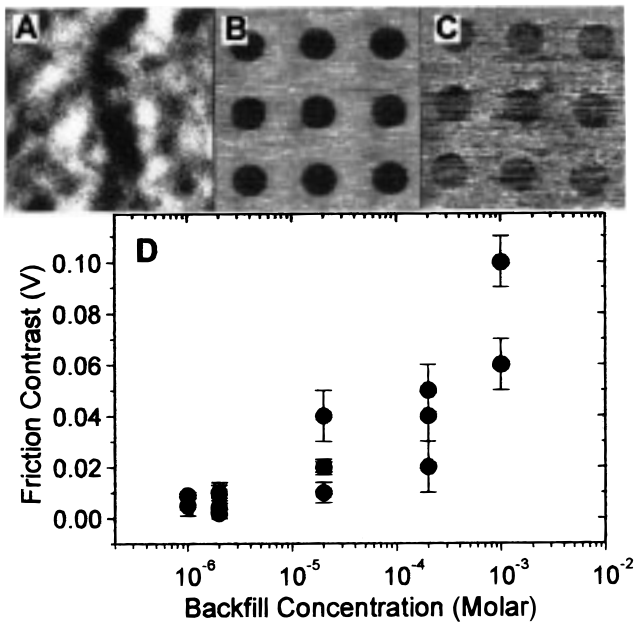

Figure 3. LFM contrast for varied solution backfill concentrations. All three AFM images are for decanethiol monolayers stamped with circles and backfilled with ethanolic solution; all are 60 μm on a side. Part A is the topography of a 1 mM backfilled sample, 3 nm full scale from black to white, and reflects the roughness of the sputtered gold surface. Parts B and C are friction images with a black-to-white full scale of 0.1 V, stamped identically and backfilled with 1 mM and 2 μM solutions, respectively. The lighter the image, the higher the friction, so the stamped regions have lower friction than solution-deposited regions. Part D indicates the average contrast as a function of the backfill solution concentration, as derived from cross-sectional cuts through the images.

be well-ordered, with a coherence length of 1500−2000 Å, and appeared to remain unaffected by the stamping process.

The connection between image contrast and domain sizes is further established in Figure 3, by LFM images in which the circles were stamped as described and the rest of the surface filled in with varying concentrations of decanethiol solution in ethanol. The stamped films were incubated in the low-concentration solutions overnight to ensure full coverage for even the 1 μM solution with an adsorption time constant of 15 min.[19,20] It has previously been shown that lower concentration solutions result in better ordered films, and this was also observed in the nonanethiol example of Figure 3.[19,20] Monolayer growth from a micromolar solution results in domain sizes as high as or higher than those seen for the stamped decanethiol monolayers, so that the phase and lateral force contrast in this case should diminish. Indeed, under identical imaging conditions, utilizing the same tip and force, the LFM contrast is less, but some contrast is still observed, as summarized in part D of Figure 3.

Conclusions

Utilizing GIXD to characterize microcontact-printed monolayers results in some new insights into the differences between stamped and solution-grown films. The local structures in the two appear to be identical, confirming previous work, but differences are observed in the defect distributions. In particular, printing with shorter length thiolate molecules results in a more ordered film than standard millimolar solution techniques, which agrees with previous observations implying that the stamped regions have a higher packing density.[8] This explains some but not all of the contrast observed in LFM for the two techniques, especially since the differences in order do not appear to extend to longer molecules. Other effects, such as the more ordered films created by increasing the concentration of stamping solution observed in NEXAFS, were not seen here, possibly because the X-ray studies are most sensitive to lateral displacements of molecules and not to intrinsic disorder due to gauche defects, although the two should be related.[9,10] It is possible that other, less correlated, defects, which would require more extensive STM studies for characterization, are present in the films without affecting the overall coherence length. There may also be effects arising from the backfilling step in stamped systems, in which some of the defects are filled in, secondary intercalation effects arise, or existing molecules are replaced. It seems clear that the stamping process itself is fairly complex, leading to unexpected degrees of order or disorder. Although we have demonstrated one variation in film properties arising from the two preparation techniques, clearly more studies are needed to elicit further variables.

Acknowledgment. This research was carried out in part at the National Synchrotron Light Source, Brookhaven National Laboratory, which is supported by the U.S. Department of Energy, Division of Materials Sciences and Division of Chemical Sciences. R.M.N. acknowledges the support of the National Institutes of Health through Grant 5T3 GM08496-04. Work at LANL was supported by LDRD funding and performed under the auspices of the U.S. Department of Energy.

LA981067R

(18) Schreiber, F.; Eberhardt, A.; Leung, T. Y. B.; Schwartz, P.; Wetterer, S. M.; Lavrich, D. J.; Berman, L.; Fenter, P.; Eisenberger, P.; Scoles, G. *Phys. Rev. B* **1998**, *57*, 12476−12481.
(19) Eberhardt, A. S. Ph.D. Thesis, Princeton University, 1997.
(20) Eberhardt, A.; Fenter, P.; Eisenberger, P. In process.